RSC Advances

PAPER

View Article Online
View Journal | View Issue

Cite this: *RSC Adv.*, 2021, **11**, 28704

A method for partitioning dissolved polycyclic aromatic hydrocarbons associated with humic substances using polyethylenimine-coated glass fiber filters†

Hisanori Iwai, *[a] Rodrigo Mundo[b] and Seiya Nagao[a]

The use of a glass fiber filter coated with polyethyleneimine (PcGF) for partitioning dissolved polycyclic aromatic hydrocarbons (PAHs) that are associated with humic substances (HSs) is reported. The PAHs pass through the PcGF, while HS-associated PAHs are trapped by electrostatic interaction between the HSs and the PcGF. Based on this strategy, free- and associated-PAHs can be separated by simple filtration. Approximately 60–90% of the deuterated benzo[*a*]pyrene (BaP-d12) that was added to the sample solutions was in the associated form with soil type HAs, while the percentages were lower in the case of aquatic HA (*ca.* 25%) and FAs (*ca.* 10–15%). Strong correlations (R^2 = 0.84–0.90) were observed between the %-association for deuterated pyrene (Pyr-d10) or BaP and the degree of HS's aromaticity (log E_{280}), regardless of the HS fractions or their origins. The separation technique was used to evaluate the association coefficient (log K_{assoc}) and the capacity (C_{assoc}) for soil type HAs based on a Langmuir adsorption model. The log K_{assoc} values were not highly dependent on the origin of the HA (*ca.* 3.5–4.5). The BaP-d12 and Pyr-d10-C_{assoc} values for the HA derived from compost were more than one order larger than the corresponding values for peat. The findings indicate that C_{assoc} values vary with the origin of the HA and affect the environmental behavior of PAHs. The present study reports on the development of a simple partitioning technique that does not require any special training and equipment.

Received 26th June 2021
Accepted 19th August 2021

DOI: 10.1039/d1ra04953d

rsc.li/rsc-advances

1 Introduction

A wide range of hydrophobic organic pollutants are released into the environment by modern industrial and agricultural activities,[1] understanding the distribution and fate of such pollutants is crucial for the scientific community and public health.[2] The influence of humic substances (HSs) on the environment is thus a major issue. HSs are complex and heterogeneous organic matter formed by the decomposition of plants, animals, and microorganisms, and they are ubiquitous as particulate or soluble forms in various environments.[3] The structural properties of HSs permit them to bind various organic compounds *via* hydrophobic interaction, as well as trace metals.[4,5]

Polycyclic aromatic hydrocarbons (PAHs), which are mainly released by the incomplete combustion of fossil fuels and organic matter, are well-known examples of hydrophobic organic pollutants.[6–8] They have mutagenic and carcinogenic characteristics,[6,7] thus making them important in regards to human health as well as other organisms.[8] Because of this, the U.S. Environmental Protection Agency (USEPA) has listed 16 such components as priority pollutants.[9] It was reported that 331–818 Gg of 16 PAHs was globally released into the atmosphere in 2007.[9] After atmospheric release, the PAHs are deposited on terrestrial and aquatic environments where the HSs then become associated with aromatic species.[4,10,11] Therefore, a knowledge of the affinity of HSs to be associated with PAHs would allow us to better understand their behavior and fate. The traditional methodology for estimating the association coefficient of HSs–PAHs involves fluorescence-quenching methods,[10,12,13] the equivalent-dialysis methods,[14] solubility enhancement methods,[15] and reversed-phase separation.[16,17] A tandem-cartridge technique was also recently proposed.[11] All of the above methods have experimental advantages and disadvantages. For example, while fluorescence quenching represents an easily and commonly used method, it frequently overestimates associability values due to quenching, such as by collision, dissolved oxygen, and inner filtration. Because of these drawbacks, it is necessary to select methods that take sample properties, experiment situations, equipment, and cost into consideration. In addition, the development of

[a]*Low-Level Radioactivity Laboratory, Institute of Nature and Environmental Technology, Kanazawa University, Nomi 923-1224, Japan. E-mail: h-iwai@se.kanazawa-u.ac.jp*

[b]*Division of Material Chemistry, Graduate School of Natural Science and Technology, Kanazawa University, Kanazawa 920-1192, Japan*

† Electronic supplementary information (ESI) available. See DOI: 10.1039/d1ra04953d

new methodologies should also have the potential for use in future studies.

As described above, HSs contain acidic functional groups, such as carboxylic acid and phenolic-OH groups, and are typically negatively charged except under strongly acid conditions. As a result, they can be adsorbed on positively charged surfaces by the electrostatic interactions. This phenomenon is a common occurrence in the natural environment. For example, metal ions are adsorbed on clay minerals and dissolved organic matter in soil and aquatic environments.[18,19] We previously reported on the functionalization of a glass fiber filter by coating it with a cationic polymer. The resulting filter was used to trap HSs on its surface by electrostatic interactions,[20] while uncharged dissolved organic matter, such as PAHs, pass through these filters. In cases where HSs are associated with the PAH fraction, they could be trapped on the filter along with HSs. It would therefore be expected that free-PAHs could be separated from HSs by filtration using a filter coated with a cationic substance. Based on this, we examined the use of a glass fiber filter as a possible separation method. Separating free-PAHs and associated-PAHs was examined by a simple filtration through a filter coated with polyethyleneimine, a cation polymer. In addition, to investigate the influence of HSs on the solubility of PAHs, three types of humic (HA) and fulvic acids (FA) from different origins (bark-compost, peat soil, and groundwater) were employed in this work. The association coefficient and capacity of HAs to associate with PAHs were examined using this electrostatic separation technique.

2 Experimental

2.1 Chemicals

Five deuterated PAHs (d-PAHs) listed in Table 1; naphthalene-d8 (Nap-d8), acenaphthene-d10 (Ace-d10), phenanthrene-d10 (Phe-d10), pyrene-d10 (Pyr-d10), and benzo[*a*]pyrene-d12 (BaP-d12) were obtained from Wako Pure Chemical Industries, Ltd., (Osaka, Japan) as environmental analysis grade materials (98% purity). PAHs are usually emitted into the environment as a mixture of various ring components; accordingly, d-PAHs were added to samples in the form of a solution of a mixture (Table 1). Anhydrous dimethyl sulfoxide (DMSO), gas chromatography grade, and polyethylenimine (PEI, average MW 1800) were also obtained from Wako (Osaka, Japan). HPLC grade acetonitrile (99.9% purity) and HLC-DISK3 filter (pore size 0.45 μm) were obtained from Kanto Chemical Co. (Tokyo, Japan). All other chemicals were obtained from Wako (Osaka, Japan) as an analytical reagent grade unless stated otherwise.

2.2 Humic substances

Hardwood bark compost (Sanyo Chip Industry Co., Ltd., Japan) and Aberdeen shire peat (Rivers Import, Japan) were used as model soil HSs, and HA and FA were extracted based on the IHSS protocols described elsewhere.[22,23] Groundwater was obtained from Mobara (Chiba, Japan) at a depth of 792–1202 m below the surface and was used as the source of aquatic HSs. HA and FA were then obtained by a XAD-8 resin technique as described in previous studies.[24,25] These humic substances were freeze-dried and stored as a powder in a UV-protected desiccator. HA and FA samples were denoted based on their origins follows; Hc (Hardwood bark compost), Ap (Aberdeen shire peat), and Mg (Mobara groundwater). For example, HcHA represents HA isolated from a hardwood bark compost.

2.3 Structural properties of the humic substances

UV-vis spectra of 20 mg L^{-1} HS diluted in 0.1 M phosphate buffer (pH 7.00) were recorded using a U-3010 spectrophotometer (Hitachi, Japan) using a 1 cm pass length quartz cuvette. The absorptivities were determined by dividing the absorbances at an arbitrary wavelength by the total organic carbon concentrations (TOC) determined by a TOC-V/CSN type TOC analyzer (Shimadzu, Japan).

Fluorescence spectra of 10 mg L^{-1} solutions of HcHA and ApHA, 1 mg L^{-1} solution of MgHA, and 0.5 mg L^{-1} solutions of FAs diluted in 0.05 M Tris–HCl buffer (pH 7.00) were measured using a fluorescence spectrometer F-7100 (Hitachi, Japan). The fluorescence properties were estimated based on the humification index (HIX) and biological index (BIX). HIX is the ratio of the integral fluorescence intensities within the emission wavelength from 400–480 nm to 330–345 nm at an excitation wavelength of 254 nm.[26] BIX is the ratio of the fluorescence intensity at 380 nm to 430 nm of the emission wavelengths which were excited at 320 nm.[27]

2.4 Preparation of PcGF and adsorption of HA

GC-50, 90 mm diameter glass fiber filters (ADVANTEC, Japan), were coated by passing 300 mL of 100 mg L^{-1} PEI in 0.1 M borate buffer (pH 8.00 ± 0.02) through them under reduced pressure followed by rinsing with 500 mL of pure water. The

Table 1 Composition of the d-PAH solution and the water solubilities of the five corresponding undeuterated PAHs

		Concentrations		
d-PAHs	Abbreviations	Mix solution (ng μL^{-1})	Sample[a] (ng L^{-1})	Water solubility[b] at 25 °C (ng L^{-1})
Naphthalene-d8	Nap-d8	3.46	1730	3.1×10^7
Acenaphthene-d10	Ace-d10	1.24	620	1.6×10^7
Phenanthrene-d10	Phe-d10	2.32	1160	1.1×10^6
Pyrene-d10	Pyr-d10	0.13	65	1.3×10^5
Benzo[*a*]pyrene-d12	BaP-d12	0.135	67.5	1.5×10^3

[a] The case of a 100 μL of d-PAHs mix was added to 200 mL of HS solution. [b] From Tobiszewski and Namieśnik (2012).[21]

resulting filter, a PEI coated glass fiber filter, is hereafter referred to as PcGF. The adsorption behavior of PEI was estimated based on the changes in TOC values, while the behavior of HSs on a PcGF was estimated by the changes in the absorbance of the filtrates at 240 nm using a U3010 spectrophotometer (Hitachi, Japan) with a 1 cm pass length quartz cuvette, but a 10 cm pass length was used in the case of a 2 mg L^{-1} solution of HA. The filtration process was carried out at a speed of approximately 3–6 mL s^{-1} unless stated otherwise.

2.5 Separation, extraction, and determination of PAHs

A 100 μL of d-PAH mix solution was added to 200 mL of a 2 mg L^{-1} solution of HS in a 0.01 M Tris aqueous buffer (pH 7.00 ± 0.02), and the resulting solution was then stirred for one hour. The sample solution was then passed through a PcGF under reduced pressure. After rinsing with pure water, the PcGF was dried under a UV-protected desiccator over silica gel for more than two days. The dried PcGF was then cut into small fragments (<1 cm × 1 cm) using ceramic scissors, the PAHs were extracted from the fragments with two portions of 20–30 mL dichloromethane by ultrasonication for 15 min.[28] The supernatant was filtered using an ADVANTEC no. 6 type filter. A 50 μL portion of DMSO was added to the eluent in order to avoid the loss of PAHs by volatilization, and dichloromethane was removed using a rotary evaporator until only the DMSO remained.[28] The remaining DMSO fraction was diluted to 1000 μL with acetonitrile, and the diluted solution was then filtered through an HLC-DISK3 type membrane disk. A 20 μL aliquot of the solution was then injected into the HPLC for the analysis of PAHs. In estimating the association ability of the samples, the above experiment was carried out with the condition that the injected volume of the d-PAH mix being varied from 0 to 400 μL into 100 mL of an HS solution (2 mg L^{-1}). In the above experiments, the concentrations range of the d-PAHs in the samples was within the range of solubility for each PAHs, and the values were much smaller than the upper solubility limits (Table 1).

The PAHs were analyzed by HPLC, as described in previous reports.[28,29] The system was comprised of an LC-20AT, CTO-20A column oven, and RF-20Axs fluorescence detector (Shimadzu, Japan). An inertsil ODS-P column (diameter 4.6 mm, length 250 mm, 5 μm, 30 °C) was employed for the separation. The wavelength pares of excitation/emission (nm) to detect PAHs were follows: 280/340 for Nap-d8, Ace-d10 and Phe-d10; 331/392 for Pyr-d10; 264/407 for BaP-d12. The mobile phase was a mixture of acetonitrile and ultrapure water operated under a gradient elution from 55–99% of acetonitrile in ultrapure water at a flow rate of 1 mL min^{-1}.

3 Results and discussion

3.1 Adsorption behavior

Fig. 1 shows the adsorption and desorption behavior of the PEI on a glass fiber filter. Approximately 0.3 mg-TOC of PEI was adsorbed on a glass fiber filter in the first 50 mL of filtration, and the adsorbed amount was saturated at about 0.4 mg-TOC per filter after an additional 150–200 mL of filtration. After passing 500 mL of aqueous PEI, pure water was then passed through the filter to desorb the PEI. The amount of desorbed PEI reached a plateau at approximately 0.1 mg-TOC after 300 mL. From these results, the mean value of the PEI adsorbed on a filter was estimated to 0.33 mg-TOC based on the difference between the TOC values of the adsorbed and desorbed PEI (Fig. 1). Thus, in subsequent experiments, the coated glass fiber filter (PcGF) was prepared by filtering 300 mL of aqueous PEI and rinsing with 300–500 mL of pure water.

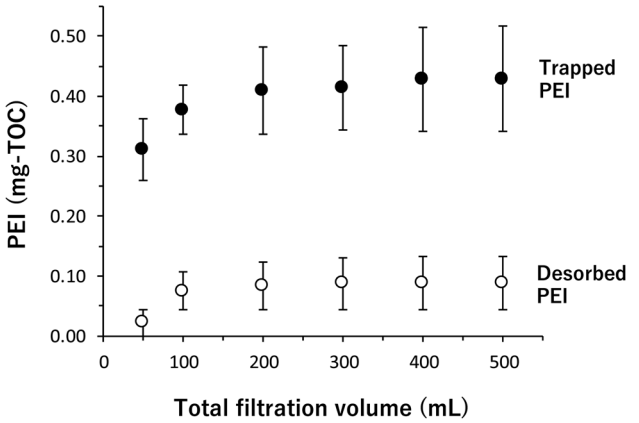

Fig. 1 The adsorption and desorption behaviors of PEI on a glass fiber filter (φ90 mm diameters GC50, ADVANTEC). The plots and error bars represent the average values and standard deviations (n = 3), respectively.

Fig. 2 shows the HS absorption behavior on a PcGF, which was investigated using aqueous HcHA (pH 7.00 ± 0.02 adjusted with 0.01 M Tris–HCl). More than 95% of the HcHA was adsorbed on the PcGF from 50–200 mL of a 2 mg L^{-1} solution of HcHA, and the ratio of adsorption (%) then decreased gradually with filtration volume (*ca.* 60% after 500 mL). In the case of 5 mg L^{-1} and 10 mg L^{-1} HcHA solution, the adsorption ratio exceeded 90% when their filtration volumes were under 100 and 50 mL, respectively. However, after filtering 500 mL of these solutions, the values decreased to approximately 38% and 20% for 5 mg L^{-1} and 10 mg L^{-1} aqueous solutions of HcHA, respectively (Fig. 2). Consequently, a reasonable filtration volume for adsorbing dissolved humic substances with a PcGF was determined to be 200 mL, 100 mL, and 50 mL filtration

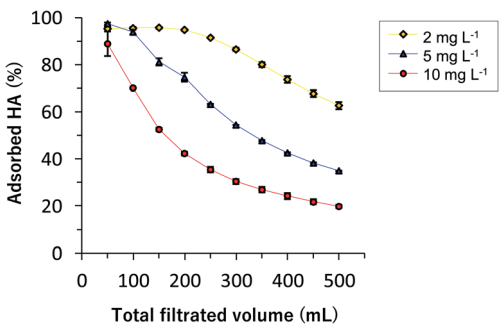

Fig. 2 The adsorption behavior in various concentrations of HcHA (2, 5, and 10 mg L^{-1} in 0.05 M Tris–HCl, pH 7.00) on the PcGF. The plots and error bars represent the average values and standard deviations (n = 3), respectively.

volumes for 2 mg L^{-1}, 5 mg L^{-1}, and 10 mg L^{-1} of humic substances, respectively.

3.2 Separation of free- and HSs-associated-PAHs

Fig. 3 shows the HPLC chromatograms for each sample extracted from the PcGF filtered solutions of HSs spiked d-PAH mix. As shown in the HS-free chromatogram (Fig. 3), no PAH peaks appeared because free-PAHs, which contain no negatively charged functional groups, pass through the PcGF. Nevertheless, a peak for BaP-d12 was observed from the PcGF in the samples cotaining HS, indicating that the BaP-d12 detected in this sample was associated species with the HSs. Nap-d8, Ace-d10, and Phe-d10 were not detected from the PcGF in the HSs and d-PAHs mix solution, suggesting that these 2–4 rings PAHs behaved as free-PAH species in the aquatic environment.

The percentage of associated Pyr-d10 and BaP-d12 were calculated from their relative areas to the corresponding values for controls, and the results are shown in Fig. 4. In all HS variants, the PAHs that were associated with HA were stronger than those for FAs. The %-associated fraction of BaP-d12 varied with the origin of HAs (*ca.* 25–92%). Although HcHA showed the highest level of association with BaP-d12 (*ca.* 92%), the value for the %-associatioin for HcFA was significantly lower (*ca.* 12%). A similar trend was observed in the case of the other HS series. Interestingly, approximately 10–15% of the added BaP-d12 was associated with FAs regardless of their origins. The %-associated BaP-d12 for MgHA was quite small compared to those of HcHA and ApHA (*ca.* 60%), suggesting that MgHA has

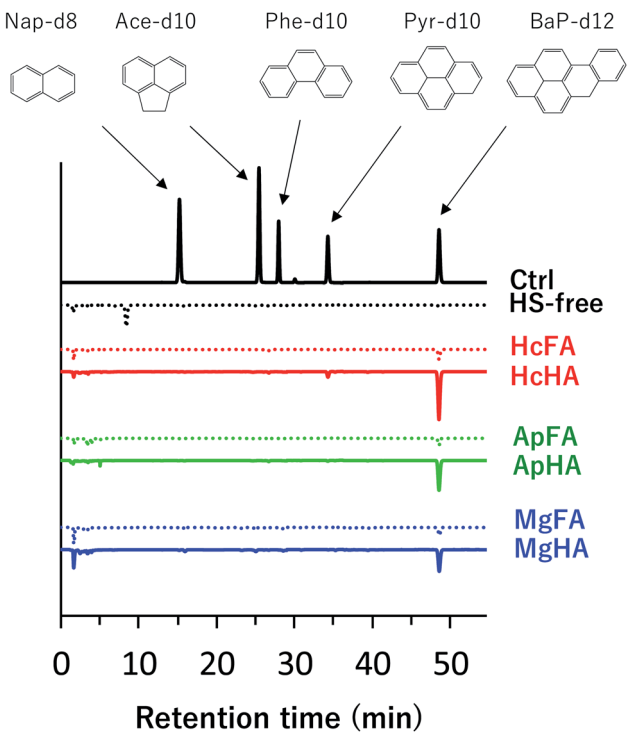

Fig. 3 HPLC chromatograms of d-PAHs extracted from the PcGF after the sample solutions had passed through the filter. The chromatogram intensities were reversed except for Ctrl to easier compare the retention time of the arbitrary peaks.

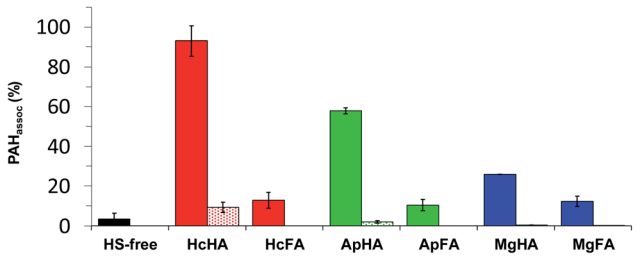

Fig. 4 The values of %-associated PAHs to HSs. Solid and meshed columns represent the cases for BaP-d12 and Pyr-d10, respectively. Hight and error bar represents the average values and standard deviations of triplicate experiments, respectively.

an FA-like character rather than that of an HA. Small amounts of associated Pyr-d10 were also observed but only in the cases of HcHA (*ca.* 8%) and ApHA (*ca.* 2%). These findings indicate that the behavior of PAH, in particular PAH molecules with larger numbers of rings, would be influenced by the presence of HA rather than the FA fraction.

3.3 Structural features and PAHs-associability of HSs

The environmental functions of HSs are closely related to their structural features. The structural features of HSs can be estimated by their UV-vis absorptivities and fluorescence properties. UV-vis spectra are shown in ESI (Fig. S1†), and the optical indexes are summarized in Table 2. The log E_{600} and log E_{280} values are correlated with the degree of condensation and aromatic component contents, respectively.[30,31] The log E_{400}/E_{600} ratio is also associated with the degree of condensation, aromatization, as well as molecular size.[32,33] HcHA had a lower log E_{400}/E_{600} ratio and higher log E_{280} and log E_{600} values, suggesting that HcHA was an extensively humified fraction that contained a highly conjugated system and aromatic components. A similar character to HcHA was found in the ApHA based on UV-vis absorptivities. The UV-vis absorptivity suggests that HcHA and ApHA had higher aromatic properties compared with the corresponding values for the FAs. The MgHA showed more of an FA-like character compared to soil-derived HAs, and the result was consistent with the reported character of aquatic humic substances.[34] The HIX value is attributed to the higher degree of humification, as evidenced by the emission wavelength derived from aromatic components that are excited by a 254 nm redshift as a result of poly-condensation.[27] BIX is also a helpful index for evaluating the bacterial derivatives in dissolved organic matter.[27,35] The BIX values for soil-derived humic substances (Hc- and Ap-series) were in the range of approximately 0.36–0.58, indicating that terrestrial organic matter was dominant, a result that is consistent with the origins of the materials (compost and peat). While that for MgHSs was about 1.0, indicating that the MgHSs were mainly composed of autochthonous matter, *i.e.*, biological by-products. These results are in agreement with the degree of humification as determined from UV-vis absorptivity measurements.

To better understand the relationship between PAH associability (%) and the characteristic of the HSs, the %-associations of BaP-d12 and Pyr-d10 for each HS sample were plotted, as

Table 2 UV-vis indexes and the atomic ratio of the HSs

		Hardwood bark compost		Aberdeenshire peat		Mobara groundwater	
		HcHA	HcFA	ApHA	ApFA	MgHA	MgFA
UV-vis indexes	log E_{400}/E_{600}	0.85	1.38	0.96	1.28	1.22	1.34
	log E_{600}	0.776	0.468	0.577	0.387	0.563	0.495
	log E_{280}	1.81	1.50	1.67	1.46	1.59	1.31
Fluorescence indexes	HIX	21.4	10.4	18.7	6.62	5.01	3.68
	BIX	0.416	0.511	0.359	0.582	1.00	0.900

shown in Fig. 5. The percentage values of associated BaP-d12 (% BaP-assoc) and Pyr-d10 (% Pyr-assoc) increased with decreasing log E_{400}/E_{600}, increasing log E_{600} and log E_{280}, and these relations were well-correlated exponentially (R^2 = *ca.* 0.85–0.93). A good relation was found for HIX to % PAH-assoc (R^2 = *ca.* 0.75–0.86). However, the plots were more spread out in the case where the *X*-axis was BIX ($R^2 < 0.35$), indicating that very low levels of bacterial by-products contributed to the PAH that was associated with humic fractions. Aromatic components in the HS structure could serve as a high-affinity association site for PAHs, as evidenced by the finding that a larger aromatic content contributed to an increase in % PAH-assoc. These findings are consistent with previously reported findings.[10,15,36] Chin *et al.* (1997) suggested that a larger molecular size could provide spaces for association with planer-shaped PAH molecules to occur.[15] HSs are supermolecular structures made up of the humification of low molecular-sized precursors; the molecular size of HSs thus increases with the degree of humification.[3,37] In addition, the aromaticity of HSs tends to increase with the humification process.[37,38] These mechanisms provide a plausible reason for the strong correlation between the % PAH-assoc *vs.* the humification indexes (log E_{600}, log E_{400}/E_{600}, and HIX). The degree of humification and aromaticity appear to be key determinants in the association of PAHs with HSs (Fig. 5).

3.4 Evaluation of the associability of PAHs–HSs

To evaluate the associability parameters, separating experiments using PcGF was performed to 200 mL of HcHA or ApHA aqueous solutions (2 mg L^{-1}, pH 7.00) injected various volumes

Table 3 Association parameters for HAs to Pyr-d10 or BaP-d12

	Pyr-d10			BaP-d12		
	log *K*	*C* (ng mg^{-1}-HA)	r^2	log *K*	*C* (ng mg^{-1}-HA)	r^2
HcHA	3.52	33.9	0.982	4.20	503	0.950
ApHA	4.21	3.10	0.948	4.46	134	0.927

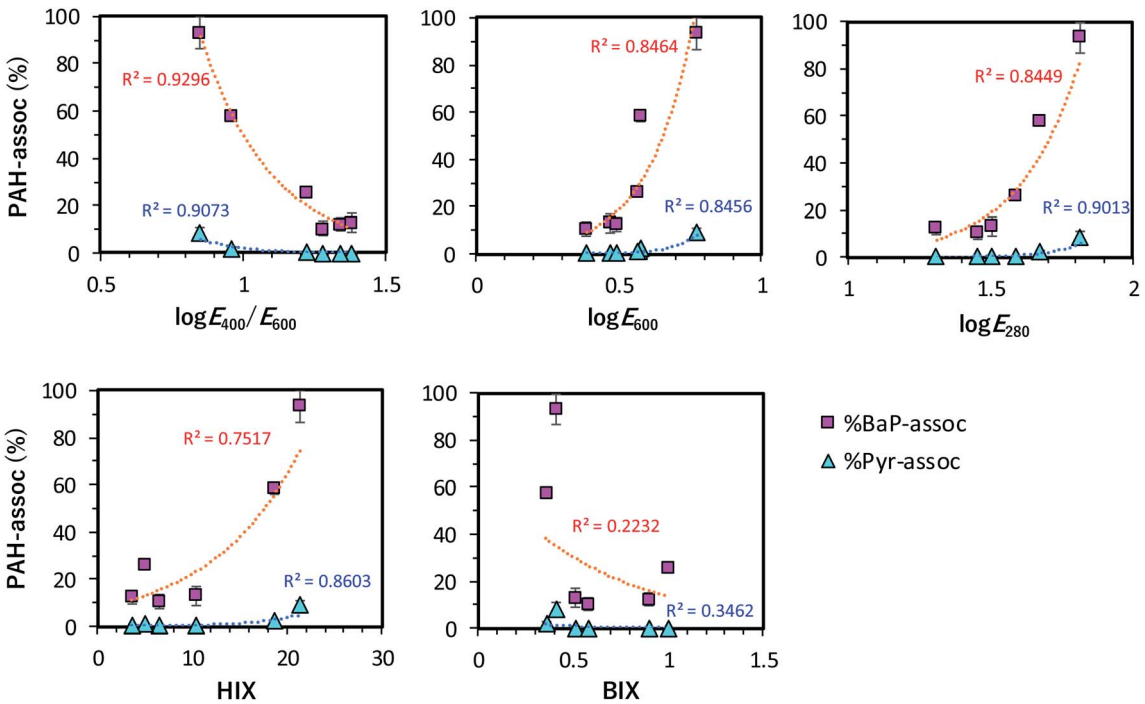

Fig. 5 The relationship between the PAH associability (%) and optical indexes.

of d-PAHs mix solution (0 to 400 μL). The relationship between free- ($[PAH]_{free}$) and associated PAHs with HA ($[PAH]_{assoc}$) are shown in Fig. 6. In all cases, the values of $[PAH]_{assoc}$ increased with increasing $[PAH]_{free}$ until they reached a plateau, and the resulting plots show a curvature suggestive of Langmuir-type adsorption. Consequently, according to the Langmuir model, the association reaction can be described as below,

$$HS + PAH \rightleftharpoons HS\text{–}PAH. \quad (1)$$

Eqn (1) is rewritten to the equilibrium below using the dimension of each concentration,

$$[HS] + [PAH]_{free} \rightleftharpoons [PAH]_{assoc}, \quad (2)$$

From eqn (2), the association coefficient, K_{assoc}, is then expressed as shown below:

$$K_{assoc} = \frac{[PAH]_{assoc}}{[HS] \times [PAH]_{free}}. \quad (3)$$

Here, the total association capacity in HS, C_{assoc}, can be defined as the sum of the unassociated and associated sites in the HS, as described below:

$$C_{assoc} = [HS] + [PAH]_{assoc}. \quad (4)$$

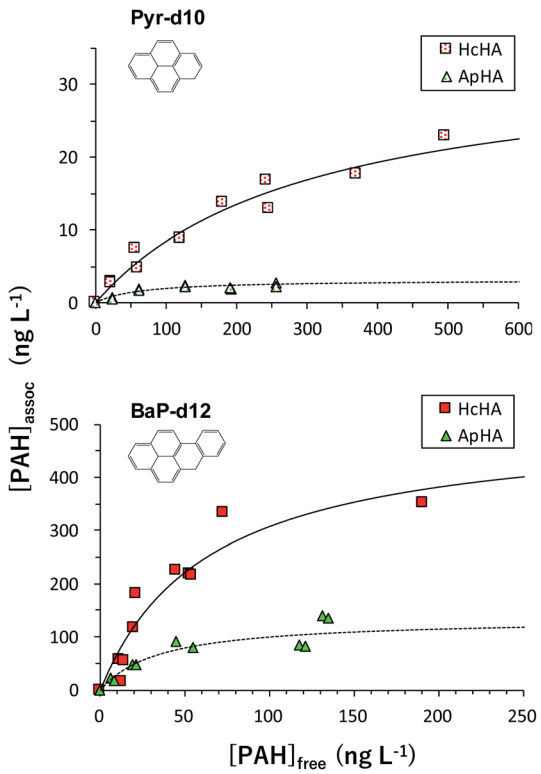

Fig. 6 Langmuir plots of $[PAH]_{free}$ *vs.* $[PAH]_{assoc}$. Upper and down are the case of Pyr-d10 and BaP-d12, squares and triangles represent the case of HcHA and ApHA, respectively.

The relationship between the concentrations of free and associated PAH with HS can then be expressed from eqn (2)–(4), as below:

$$[PAH]_{assoc} = \frac{K_{assoc} \times C_{assoc} \times [PAH]_{free}}{1 + K_{assoc} \times [PAH]_{free}}. \quad (5)$$

The values of K_{assoc} and C_{assoc} were estimated by fitting eqn (5) to the experimental plots using the least squared method. The fitting for eqn (5) is shown as solid and broken lines in Fig. 6. The fitting curves were fitted well to the plots ($r^2 = 0.923$–0.982), suggesting that a Langmuir-type adsorption reaction is a suitable concept for explaining the association between the PAHs and HAs. Based on this concept, the results indicate that HAs contain a specific association site for PAHs, resulting in a monolayer molecular association. The evaluated associability values were summarized in Table 3. The values of log K_{assoc} for ApHA (*ca.* 4.2 for Pyr-d10, 4.5 for BaP-d12) were slightly larger than those for HcHA (*ca.* 3.5 for Pyr-d10, 4.2 for BaP-d12). These values, however, were slightly lower compared with values obtained using the fluorescence quenching method: 4.3 or 4.96 for river HA-Pyr,[13,15] the reverse phase method: 4.5–4.6 for compost soil-benzo(*e*)pyrene,[17] and the equilibrium dialysis method: 4.9–6.3 for dissolved organic matter-BaP.[36] The separation under flow conditions (3–6 mL s^{-1}) permitted the labile species of PAH-assoc to be desorbed from the HSs that were trapped on the PcGF, and this is considered to be one of the causes of the underestimation of K_{assoc} compared to the other methods.[13,15,17] In general, in field studies, PAHs are fractionated into particulate and dissolved-phase species, and the particulate phase is defined as the fraction trapped on a glass fiber filter (>0.5 μm).[28,29] The particulate phase PAHs is regarded as the species adsorbed on the surface of the organic or inorganic particle cores. The experimental conditions used here are the same as that of field studies; the method proposed here was anticipated to be a useful approach to investigating the influence of the associability of the particulate surface on determining the distribution of PAHs in aquatic environment surveys. The C_{assoc} values varied depending on the sample; in both cases of Pyr and BaP, the HcHA contained a significantly larger C_{assoc} than that for ApHA. This result is in agreement with the highest %-PAH_{assoc} for HcHA showed in Fig. 4. The high aromaticity of HcHA would permit it to have a large number of binding sites for PAHs. From these results, the PAH appears to be associated with a specific site in the HA molecules, and the log K_{assoc} values were in the range of *ca.* 4–6, regardless of the origin of the HSs.[13,15,17,18] However, the values for C_{assoc} varied significantly, depending on the origin of the HA. We, therefore, conclude that the adsorption capacity is the most important factor that significantly influences the behavior of PAHs in the environment rather than the log K_{assoc} value.

4 Conclusions

This study produced a PcGF method, which uses a glass fiber filter coated with polyethyleneimine (PEI), available for the separation of dissolved organic matter with electrostatic

interactions. The preparation and use of the method did not require any special experimental techniques nor expensive materials. The PcGF was easily prepared by filtration of PEI aqueous and pure water. The resulted PcGF succeeded in trapping dissolved PAHs associated with humic substances (HSs), because the associated PAHs electrostatically interacted with PcGF using the negative charge of HSs, while free-PAHs pass through the filter. As a result, 60–80% of the added BaP-d12 was associated with the soil type HA fraction; however, significantly smaller %-association values were observed for the aquatic HA and FA fractions. The percentage association values were strongly correlated with the degree of aromaticity ($\log E_{280}$) for humic substances, regardless of their origins and fractions.

In addition, the PcGF method was applied to estimate the associability of HSs with PAHs in aqueous. The Langmuir adsorption isotherm was fitted well to the relationship between the concentrations of free- and associated-PAHs (Pyr-d10 or BaP-d12), indicating that PAHs are associated with a specific site in the HSs. The values of $\log K_{\mathrm{assoc}}$ and C_{assoc} were then evaluated by fitting the isotherm. The $\log K_{\mathrm{assoc}}$ value was approximately 3.5–4.5, while C_{assoc} was significantly dependent on the origins of the HAs, suggesting that the PAHs behavior would be influenced by the magnitude of C_{assoc} value rather than $\log K_{\mathrm{assoc}}$ of HSs in the environment.

Conflicts of interest

The authors declare no conflicts of interest associated with this manuscript.

Acknowledgements

This work was financially supported by the Chozen project of Kanazawa University.

References

1 D. A. Backhus, C. Golini and E. Castellanos, *Environ. Sci. Technol.*, 2003, **37**, 4717–4723.
2 T. Rasheed, S. Shafi, M. Bilal, T. Hussain, F. Shar and K. Rizwan, *J. Mol. Liq.*, 2020, **318**, 113960.
3 G. R. Aiken, D. M. McKnight, R. L. Wershaw and P. MacCarthy, *Humic Substances in Soil, Sediment, and Water*, ed. G. R. Aiken, D. M. McKnight, R. L. Wershaw and P. MacCarthy, John Wiley & Sons, New York, 1985, pp. 1–12.
4 T. L. ter Laak, M. A. Ter Bekke and J. M. Hermens, *Environ. Sci. Technol.*, 2009, **43**, 7212–7217.
5 Y. Laor and M. Rebhun, *Environ. Sci. Technol.*, 2002, **36**, 955–961.
6 K. H. Kima, S. A. Jahan, E. Kabir and R. J. C. Brown, *Environ. Int.*, 2013, **60**, 71–80.
7 B. K. Behera, A. Das, D. J. Sarkar, P. Weerathunge, P. K. Parida, B. K. Das, P. Thavamani, R. Ramanathan and V. Bansal, *Environ. Pollut.*, 2018, **241**, 212–233.
8 E. B. Balcioğlu, *Toxin Rev.*, 2016, **35**, 98–105.
9 H. Shen, Y. Huang, R. Wang, D. Zhu, W. Li, G. Shen, B. Wang, Y. Zhang, Y. Chen, Y. Lu, H. Chen, T. Li, K. Sun, B. Li, W. Liu, J. Liu and S. Tao, *Environ. Sci. Technol.*, 2013, **47**, 6415–6424.
10 V. Perminova, N. Y. Grechishcheva and V. S. Petrosyan, *Environ. Sci. Technol.*, 1999, **33**, 3781–3787.
11 N. Li and H. K. Lee, *Anal. Chem.*, 2000, **72**, 5272–5279.
12 T. D. Gauthier, E. C. Shane, W. F. Guerin, W. R. Seitz and C. L. Grant, *Environ. Sci. Technol.*, 1986, **20**, 1162–1166.
13 M. A. Schlautman and J. J. Morgan, *Environ. Sci. Technol.*, 1993, **27**, 961–969.
14 Y. Chin and J. Weber Jr, *Environ. Sci. Technol.*, 1989, **23**, 976–984.
15 Y. P. Chin, G. R. Aiken and K. M. Danielsen, *Environ. Sci. Technol.*, 1997, **31**, 1630–1635.
16 P. F. Landrum, S. R. Nihart, B. J. Eadle and W. S. Gardner, *Environ. Sci. Technol.*, 1984, **18**, 187–192.
17 B. Raber and I. Kögel-Knabner, *Eurasian J. Soil Sci.*, 1997, **48**, 443–455.
18 E. Tipping, *Cation Binding by Humic Substances*, Cambridge University Press, Cambridge, 2002.
19 M. K. Uddin, *Chem. Eng. J.*, 2017, **308**, 438–462.
20 H. Iwai, *Anal. Sci.*, 2019, **35**, 783–787.
21 M. Tobiszewski and J. Namieśnik, *Environ. Pollut.*, 2012, **162**, 110–119.
22 H. Iwai, M. Fukushima, M. Yamamoto, T. Komai and Y. Kawabe, *J. Anal. Appl. Pyrolysis*, 2013, **99**, 9–15.
23 H. Iwai, *Anal. Sci.*, 2017, **33**, 1231–1236.
24 E. M. Thurman and R. L. Malcolm, *Environ. Sci. Technol.*, 1981, **15**, 463–466.
25 S. Nagao, Y. Sakamoto, R. R. Rao and N. Fujitake, *Humic Substances Research*, 2009, **5**, 9–17.
26 A. Zsolnay, E. Baigar, M. Jimenez, B. Steinweg and F. Saccomandi, *Chemosphere*, 1999, **38**, 45–50.
27 A. Hugueta, L. Vachera, S. Relexansa, S. Saubussea, J. M. Froidefondc and E. Parlantia, *Org. Geochem.*, 2009, **40**, 706–719.
28 R. Mundo, T. Matsunaka, H. Iwai, S. Ogiso, N. Suzuki, N. Tang, K. Hayakawa and S. Nagao, *Int. J. Environ. Res. Public Health*, 2020, **17**, 904.
29 E. G. Nagato, F. Makino, H. Nakase, S. Yoshida and K. Hayakawa, *Mar. Pollut. Bull.*, 2019, **138**, 333–340.
30 Y. P. Chin, G. Aiken and E. O'Loughlin, *Environ. Sci. Technol.*, 1994, **28**, 1853–1858.
31 M. Fuentes, G. González-Gaitano and J. M. García-Mina, *Org. Geochem.*, 2006, **37**, 1949–1959.
32 N. Gressel, A. E. McGrath, J. C. McColl and R. F. Power, *Soil Sci. Soc. Am. J.*, 1995, **59**, 1715–1723.
33 Z. Droussi, V. D'Orazio, M. Hafidi and A. Ouatmane, *J. Hazard. Mater.*, 2009, **163**, 1289–1297.
34 L. Aristilde and G. Sposito, *Environ. Toxicol. Chem.*, 2013, **32**, 1467–1478.
35 M. Ateia, J. Ran, M. Fujii and C. Yoshimura, *Int. J. Environ. Sci. Technol.*, 2017, **14**, 867–880.
36 J. F. McCarthy, L. E. Roberson and L. W. Burrus, *Chemosphere*, 1989, **12**, 1911–1920.
37 M. Fuentes, R. Baigorri, G. González-Gaitano and J. M. García-Mina, *Org. Geochem.*, 2007, **38**, 2012–2023.
38 X. He, B. Xi, Z. Wei, X. Guo, M. Li, D. An and H. Liu, *Chemosphere*, 2011, **82**, 541–548.